

### Nonlinear-response effects in stochastic resonance

Hu Gang

*Institut für Theoretische Physik und Synergetik, Universität Stuttgart, D-7000 Stuttgart 80, Germany  
and Department of Physics, Beijing Normal University, Beijing 100875, People's Republic of China*

H. Haken and C. Z. Ning

*Institut für Theoretische Physik und Synergetik, Universität Stuttgart, D-7000 Stuttgart 80, Germany*

(Received 17 July 1992)

Nonlinear-response effects in stochastic resonance are investigated. An analytic solution is obtained in the framework of the adiabatic approximation. It is found that the input signal strength plays an important role in affecting the stochastic resonance behavior. Our analytic predictions fit well both numerical calculations and experimental results.

PACS number(s): 05.40.+j, 05.20.-y

The problem of stochastic resonance (SR) has attracted much attention in the past decade [1-12]. Up to now most of the theoretical analyses, apart from certain numerical works, are mainly based on perturbation theory and linear-response theory. Many experimental and numerical results strongly indicate, however, that the nonlinear response of a system to the input signal plays an important role in the SR problem [13,14]. For instance, the SR noise strength (i.e., the noise strength at which the output signal takes its maximum value) may decrease as the input signal strength increases [14], and the SR amplification ratio (i.e., the ratio of the output signal strength to that of the input) may be considerably modified by varying the input signal strength. These phenomena cannot be understood on the basis of linear-response theory because in the linear regime the input signal strength is irrelevant to the SR problem. The main purpose of this paper is to give an effective approach for describing the main nonlinear-response characteristics of the SR at sufficiently small frequency of the input signal. For considerations beyond the small-frequency (adiabatic) limit we refer the reader to [15,16].

Let us start from the following bistable model which has been extensively investigated [6-14]:

$$\dot{x} = ax - x^3 + A \cos(\Omega t + \theta) + \Gamma(t), \tag{1}$$

$$\langle \Gamma(t) \rangle = 0, \quad \langle \Gamma(t)\Gamma(t') \rangle = 2D\delta(t-t'), \tag{2}$$

which is equivalent to the Fokker-Planck equation (FPE) [17]

$$\frac{\partial p(x,t)}{\partial t} = -\frac{\partial}{\partial x} [ax - x^3 + A \cos(\Omega t + \theta)]p(x,t) + D \frac{\partial^2 p(x,t)}{\partial x^2}. \tag{3}$$

Using the adiabatic approximation McNamara and Wiesenfeld [6] proposed a two-state model to considerably simplify Eq. (3). They obtained

$$P_s(\omega) = \delta(\omega - \Omega) \frac{\pi A^2 a^2 \lambda_1^2}{2D^2(\lambda_1^2 + \Omega^2)}, \tag{4}$$

$$\mathcal{R} = \frac{\pi A^2 a \lambda_1}{4D^2}, \tag{5}$$

$$\lambda_1 = [ |U''(0)| |U''(\sqrt{a})| ]^{1/2} \exp \left[ \frac{-\Delta U}{D} \right] / \pi,$$

$$U(x) = -\frac{a}{2}x^2 + \frac{1}{4}x^4, \quad \Delta U = U(0) - U(\sqrt{a}),$$

where  $P_s$  is the spectral intensity of the signal and  $\mathcal{R}$  the signal-to-noise ratio in the output [6,7]. This result is based on the linear-response theory. The two-state model has grasped the essential point in the original continuous bistable system. The adiabatic approximation fits many practical situations very well. For instance, in our experiment [12,13] we can easily realize the condition that the relaxation time in each basin of attractors is negligibly smaller than the period of the input, and than the hopping time between the two basins, i.e.,

$$\frac{1}{a} \ll \frac{1}{\Omega}, \frac{1}{\lambda_1}. \tag{6}$$

Therefore, in this paper we stick to the adiabatic approximation (for the fundamental ideas of the adiabatic approximation, cf. Refs. [18,19]), while taking into account the nonlinear effects with respect to  $A$ . However, the effects of the continuous bistable system will be taken into account, instead of considering the simple two-state model.

The evolution of the system can be separately investigated in two time scales: a fast and a slow time scale. The fast scale corresponds to the relaxation in a single basin of attractor ( $1/a$  time scale) and the slow one is related to the transition probability between the two potential wells ( $1/\Omega$  and  $1/\lambda_1$  time scale). Since the probability transition rate can be neglected in comparison with the relaxation rate, the local asymptotic solution of Eq. (3) can be regarded as valid all the time when we consider

the evolution on the slow time scale. Therefore, we have

$$p(x, t) \approx \begin{cases} \frac{n_+(t)}{N_+(t)} \exp\left[\frac{-\bar{U}(x)}{D}\right], & x > x_u, \\ \frac{n_-(t)}{N_-(t)} \exp\left[\frac{-\bar{U}(x)}{D}\right], & x < x_u, \end{cases} \quad (7)$$

where we have used the notation

$$\bar{U}(x, t) = U(x) - Ax \cos(\Omega t + \theta). \quad (8)$$

$x_u(t)$  is one of the three solutions of

$$ax(t) - x^3(t) + A \cos(\Omega t + \theta) = 0. \quad (9)$$

The other two solutions read as  $x_+(t)$ ,  $x_-(t)$ , satisfying  $x_-(t) < x_u(t) < x_+(t)$ .  $N_\pm(t)$  are normalization factors  $N_\pm(t) = \pm \int_{x_\pm}^{\pm\infty} \exp[-\bar{U}(x)/D] dx$ . In Eq. (7),  $n_+(t)$  and  $n_-(t)$  are the total probabilities in the right and the left basins, respectively, which can be determined by the master equation

$$\dot{n}_\pm(t) = -W(t)n_\pm(t) + T_\mp(t). \quad (10)$$

We have  $n_-(t) = 1 - n_+(t)$ ,  $W(t) = T_+(t) + T_-(t)$ . The transition rates  $T_+(t)$  and  $T_-(t)$  are determined by the local asymptotic distribution equation (7) as

$$T_\pm(t) = \frac{[\lambda_u \lambda_\pm]^{1/2}}{2\pi} \exp\left[\frac{-\Delta\bar{U}_\pm(t)}{D}\right],$$

$$\Delta\bar{U}_\pm(x) = \bar{U}(x_u, t) - \bar{U}(x_\pm, t), \quad (11)$$

$$\lambda_\pm = \left. \frac{d^2U(x)}{dx^2} \right|_{x=x_\pm(t)},$$

$$\lambda_u = - \left. \frac{d^2U(x)}{dx^2} \right|_{x=x_u(t)}.$$

The solution of Eq. (10) can be easily worked out and given by

$$n_+(t) = S(t) \left[ n_+(t_0) + \int_{t_0}^t T_-(t') S^{-1}(t') dt' \right], \quad (12)$$

$$S(t) = \exp\left[-\int_{t_0}^t [T_+(t') + T_-(t')] dt'\right]. \quad (13)$$

$x_u$  corresponds to the maximum of the potential while  $x_+$  and  $x_-$  correspond to the other two solutions. It should be emphasized that, in Eq. (9), the modification of the potential wells by the periodic signal needs to be taken into account, because for large  $A$  this modification changes the system's response considerably. There is a turning point of  $A_c \approx \sqrt{4/27}$ . As  $A > A_c$ , in a certain time interval Eq. (9) has only a single real solution corresponding to the unique minimum of the potential. For such a large  $A$  the above physical picture is no longer valid, as a result this system does not show any SR phenomenon. Thus we only consider the case of  $A < A_c$ . In Eq. (11) we do not take into account the probability transition due to the motion of  $x_u(t)$ , because this transition rate is proportional to  $\Omega$  which is negligibly smaller than the rate included in (11). Since  $D \ll 1$ , the major portion of probability in each basin is centered at the minimum point of the potential. Hence, a Gaussian approximation of the local distribution is reasonable. This approximation leads to simpler expression

$$p_\pm(x, t) \approx n_\pm(t) \left(\frac{\lambda_\pm}{2\pi D}\right)^{1/2} \exp\left[-\frac{\lambda_\pm [x - x_\pm(t)]^2}{2D}\right], \quad (14)$$

where  $p_+(x, t)$  and  $p_-(x, t)$  are the probability distributions in the slow time scale in the intervals  $x > x_u$  and  $x < x_u$ , respectively. If we further consider the evolution in the fast time scale, i.e., consider the relaxation from a given  $\delta$  function  $p(x, t_0) = \delta(x - x_0)$ ,  $x_0 > x_u(t_0)$ , the probability distribution in each basin can be specified by

$$p(x, t | x_0, t_0) \approx n_+(t) \left(\frac{\lambda_+(t)}{2\pi D}\right)^{1/2} \exp\left[-\frac{\lambda_+(t) \{x - x_+(t) - [x_0 - x_+(t)] \exp[-\lambda_+(t_0)(t - t_0)]\}^2}{2D}\right], \quad x > x_u,$$

$$\approx n_-(t) \left(\frac{\lambda_-(t)}{2\pi D}\right)^{1/2} \exp\left[-\frac{\lambda_-(t) [x - x_-(t)]^2}{2D}\right], \quad x < x_u, \quad (15)$$

with  $n_+(t_0) = 1$ ,  $n_-(t_0) = 0$ . The solution for  $x_0 < x_u(t_0)$  can be obtained from Eq. (15) by replacing all the subscripts  $+$ ,  $-$  by  $-$ ,  $+$ , respectively. The solutions (12) and (15) describe the entire evolution from any initial distribution to the asymptotic state, keeping the leading order of  $\Omega$  and  $D$  in all time scales.

From Eq. (15) we can easily calculate the autocorrelation function

$$G(\tau) = \overline{\langle x(t_0 + \tau)x(t_0) \rangle}_\infty$$

$$= \lim_{t_0 \rightarrow \infty} \frac{\Omega}{2\pi} \int_{t_0}^{t_0 + 2\pi/\Omega} dt_0 \int \int dx dy xyp(x, t_0 + \tau | y, t_0)p(y, t_0)$$

$$= G_+(\tau) + G_-(\tau), \quad (16)$$

$$G_+(\tau) = \frac{\Omega}{2\pi} \int_0^{2\pi/\Omega} dt_0 \{ n_{++}(\tau, t_0) \hat{n}_+(t_0) [x_+(t_0 + \tau)x_+(t_0) + \frac{D}{\lambda_+(t_0 + \tau)} \exp(-\lambda_+(t_0)\tau)]$$

$$+ [1 - n_{++}(\tau, t_0)] \hat{n}_+(t_0) x_+(t_0) x_-(\tau + t_0) \},$$

where  $\hat{n}_+(t_0)$  represents the nondamping part in  $n_+(t_0)$ , and  $n_{++}(\tau, t_0)$  denotes  $n_+$  at  $\tau+t_0$  when  $n_+(t_0)=1$ .  $G_-(\tau)$  can be obtained from  $G_+(\tau)$  by replacing the subscripts  $+, -$  by  $-, +$ , respectively. From Eq. (16) we obtain the signal amplification as follows:

$$\beta = \lim_{\tau \rightarrow \infty} \frac{2\Omega}{\pi A^2} \int_{\tau}^{\tau+2\pi/\Omega} G(\tau) \exp\{-i\Omega\tau\} d\tau. \quad (17)$$

The autocorrelation function equation (16) represents the essential advances with respect to Ref. [6] in the following aspects.

(i) We do not consider any approximation with respect to  $A$ . Thus, the information of nonlinear response has been entirely retained. It will be shown that these nonlinear effects considerably change the behavior of the system, and enable us to understand the phenomena mentioned at the beginning of this paper.

(ii) The variation of the basin structure of the bistable system due to the periodic force has been taken into account. We even have considered the motion within a basin. Therefore, the essence of a continuous variable of the bistable system has been taken into account. Our solution will be shown to fit exact numerical solutions and experimental results better than the pure two-state model.

Now let us show what we may achieve from the analytic solution (16). In all the following figures we fix  $a=1$ ,  $\Omega=0.01$ . In Fig. 1 we plot  $\beta$  against  $D$  for  $A=0.01$  and  $0.2$ . Increasing  $A$  may push the peak towards the small  $D$ . The curve for  $A=0.01$  is identical to the linear-response result, Eq. (4). However, for relatively larger  $A$  ( $A=0.2$ ) the linear response fails. On the curve for  $A=0.2$  in Fig. 1 the amplification quantity  $\beta$  is considerably reduced from that for  $A=0.01$ . It is remarkable that our plots represent well the influence by  $A$  and recover the numerical result with very good precision (see Fig. 1 in [14]). In Fig. 2 the solid curve plots the  $D_{SR}$  (i.e., the position of the peak of the  $\beta$ - $D$  curve) against  $A$ . Apart from the region  $A \approx A_c \approx 0.38$ , our plots are in qualitative agreement with the experimental results (see Fig. 10 in [13]). In the regime about  $A_c$ , the condition

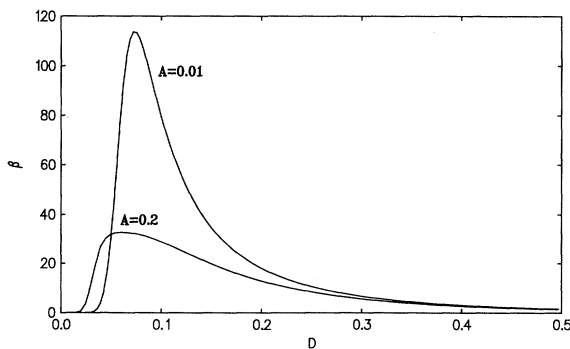


FIG. 1.  $\beta$  vs  $D$ .  $a=1$ ,  $\Omega=0.01$  ( $\Omega$  and  $a$  are not changed in all the following figures). The curve of  $A=0.01$  recovers the result of linear-response theory, while that of  $A=0.2$  perfectly reproduces the numerical result in Ref. [14].

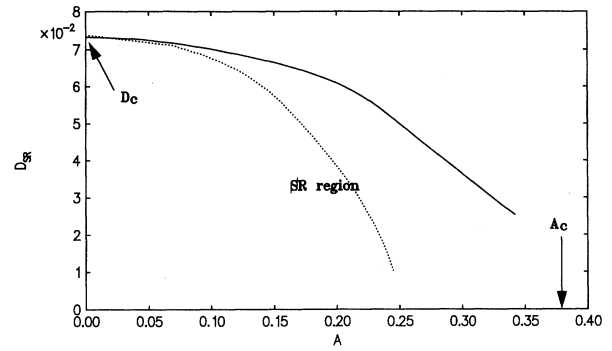


FIG. 2. The  $D_{SR}$  plotted against  $A$ . This figure is very similar to the experimental plots in Fig. 10 of Ref. [13]. The approximation is not valid at  $A \approx A_c$ . The reasonable curve should cross the point ( $A=A_c, D=0$ ). The dotted curve gives the result of the two-state model.

for our two-time-scale argument is certainly broken. The correct curve should cross the point ( $A=A_c, D=0$ ) since at  $A > A_c$  the regular switchings can be realized in the absence of noise, and then adding noise is certainly not favorable for the output signal. For  $A > A_c$  or  $D > D_c$  no SR can be found. Thus, the SR phenomenon is restricted in the SR region. The dotted curve in Fig. 2 has the same meaning as the solid one while the data are collected from the calculation of the two-state model, i.e., without considering the effects of the continuous variable. The dotted line is very close to the solid curve for small  $A$ , while considerably deviates from it for large  $A$ . The dotted curve should intersect with the  $A$  axis at  $A=0.25$  rather than  $A=A_c$ .

In Fig. 3 we plot  $\beta$  against  $A$  for various  $D$  values. For  $D > D_c$  (e.g.,  $D=0.1$ ) we find that  $\beta$  decreases monotonously by increasing  $A$ . However, as  $D < D_c$  (e.g.,

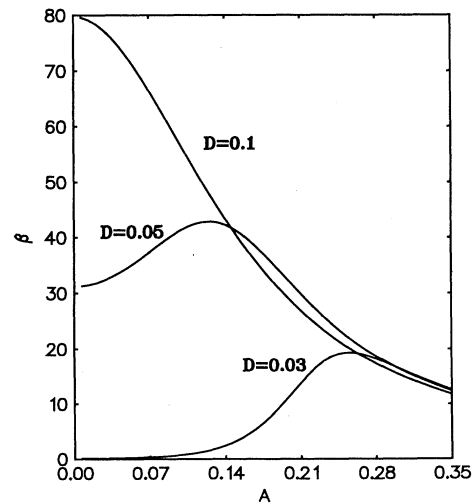


FIG. 3.  $\beta$  plotted vs  $A$  for given  $D$ 's. Stochastic resonance-like behavior is apparent for relatively small  $D$  (e.g.,  $D=0.05, 0.03$ ).

$D=0.05, 0.03$ ) one may again find a peak on the  $\beta$ - $A$  curves. These curves show the SR phenomenon with respect to the signal strength. To our knowledge, this kind of behavior is analytically predicted for the first time in the present paper on the basis of nonlinear-response theory. In Fig. 4, we again plot  $\beta_M$  vs  $A$ , with  $\beta_M$  being the maximum value of the  $\beta$ - $D$  curve for a given  $A$ . Then, we find that the amplification ratio decreases monotonously by increasing  $A$ . This fact agrees with all the numerical calculations and the experimental observations available up to date.

Since the SR phenomenon essentially relies on the optimal switching between the two basins, the hopping rate  $\lambda_1$  certainly plays a very important role in affecting the SR behavior. An important point for the nonlinear response is that the hopping rate depends on both  $D$  and  $A$ . Figure 5 shows the level curves  $\lambda_1(D, A) = (\Omega/2\pi) \int_0^{2\pi/\Omega} W(t) dt = 0.01$  and  $0.02$ . As can be seen,  $\lambda_1$  is indeed modified by changing  $A$ . Increasing  $A$  may increase the hopping rate, which turns out to be the key point for understanding the nonlinear-response effects. Especially, for  $A$  close to  $A_c$ , a slight change of  $A$  may dramatically change  $\lambda_1$ . Our model is still unable to show the behavior of  $\lambda_1$  in the vicinity very close to  $A_c$ . All the level curves should cross the point ( $A = A_c, D = 0$ ), since at  $A > A_c$  the regular switching takes place, and then the hopping rate should approach infinity (measured in slow time scale) as Eq. (9) has only a single solution. The striking resemblance between Figs. 2 and 5 strongly indicates that the SR behavior is closely related to the behavior of the hopping rate.

In all these figures we concentrate on the amplification ratio  $\beta$ . An important quantity in the study of SR is the so-called signal-to-noise ratio  $\mathcal{R}$  [6,7]. In this paper we can only give some brief discussions in this respect. From Eq. (16) one can calculate spectra of both output signal and noise. Thus, an analytic result of  $\mathcal{R}$  can be also obtained in the framework of the nonlinear-response theory. Two facts are already clear from the structure of Eq. (16) without specifying the concrete form of the solution. First,  $\mathcal{R}$  obtained by the two-state model, Eq. (5), has an unreasonable behavior that the  $\mathcal{R}$  approaches zero

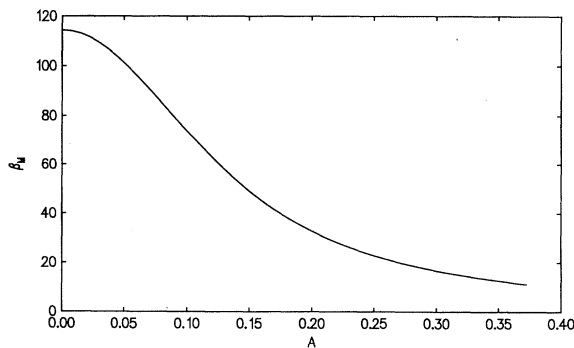


FIG. 4.  $\beta_M$  (the maximum  $\beta$  value on the  $\beta$ - $D$  curve for the given  $A$ ) plotted against  $A$ . As observed by experiments and numerical works,  $\beta_M$  monotonously decreases as  $A$  increases.

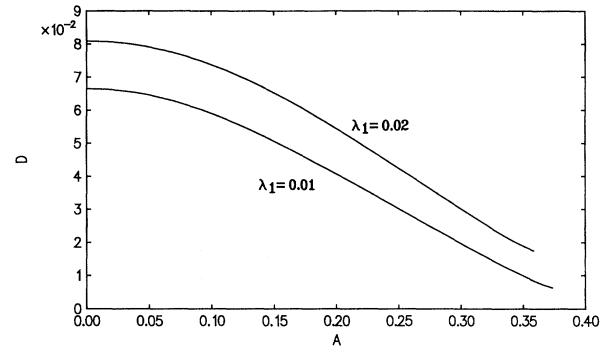


FIG. 5. The level curves of  $\lambda_1(A, D)$  in the  $A$ - $D$  plane. The resemblance of this figure to Fig. 2 is striking.

as  $D$  goes to zero. This shortcoming can be overcome in our analysis by considering the motion within a basin. As  $D \rightarrow 0$ , the noise part of (16) vanishes while the signal part does not because  $x_{\pm}(t)$  oscillates due to the input signal. Thus, the  $\mathcal{R}$  must reasonably approach infinity as  $D \rightarrow 0$  in our case. Second, in experiments we found that increasing the input signal may result in an increase of the output noise [i.e., there is a huge peak in the  $N$  (output noise)- $A$  curve, see the solid curve in Fig. 7 of Ref. [13]]. This peculiar phenomenon can never be explained by the linear-response theory [6,11]. However, from the level curves in Fig. 5, the mechanism of this seemingly peculiar behavior can be clearly understood. For small  $\Omega$  and small  $D$  the major part of the noise correlation spectrum at  $\Omega$  can be (roughly) expressed as  $N \propto \lambda_1 / (\lambda_1^2 + \Omega^2)$ . Fixing  $D$  to a small value, one may increase  $\lambda_1$  by increasing  $A$ . At a certain  $A$  the hopping rate may cross the value  $\lambda_1 = \Omega$ , and then the output noise may have a peak about it. A detailed discussion about these aspects will be published elsewhere.

At the end of this paper it is interesting to make some remarks about the adiabatic approximation. Actually, there are different definitions of adiabatic approximation. Jung and Hänggi required the following conditions [14]:

$$\Omega \ll \lambda_1, \lambda_2, \lambda_3, \dots \quad (18)$$

In this case, the asymptotic solution of Eq. (3) can be approximately expressed in the form

$$p(x, t) = N(t) \exp \left[ -\frac{\bar{U}(x)}{D} \right], \quad (19)$$

where  $N(t)$  is the normalization factor. The second definition requires Eq. (6) [6]. In the former case the global distribution can be obtained adiabatically. In the latter case, the adiabatic elimination procedure can be only used in the local evolution in each potential basin. The probability balance between the two basins, like Eq. (19), cannot be obtained in a straightforward manner. It is emphasized that the solution (7) can never approach (19) as  $\lambda_1$  is sufficiently small even if  $t \rightarrow \infty$ , though the shapes of local distributions in both cases are identical. A simple matching procedure may unify the solutions in different parameter regions. Since  $\Omega \ll a$ , we can easily

find the hopping rate satisfying the condition  $\Omega \ll \hat{\lambda}_1(A, D) \ll a$ . For instance, we can simply define  $\hat{\lambda}_1 = \sqrt{a\Omega}$ . At this hopping rate both conditions (6) and (18) are satisfied. Hence we can match the two solutions to a unified one as  $p(x, t) = [1/(1+\alpha)]p_1(x, t) + [\alpha/(1+\alpha)]p_2(x, t)$ , where  $\alpha = \lambda_1/\sqrt{a\Omega}$ , and  $p_1(x, t)$  and  $p_2(x, t)$  are the asymptotic solutions given by (7) and (19), respectively.

In Ref. [13], some experimental data were found in conceptual contradiction with the results obtained by the adiabatic approximation. This contradiction leads the

authors to the conclusion that the observations are beyond the interpretation of the adiabatic framework. Now it is clear that the main experimental features can be satisfactorily explained in the framework of the adiabatic approximation if we fully consider nonlinear responses and the effects of continuous variable of the bi-stable system.

This work was partially supported by the Deutsche Forschungsgemeinschaft.

- 
- [1] R. Benzi, A. Sutera, and A. Vulpiani, *J. Phys. A* **14**, 453 (1981).
- [2] R. Benzi, G. Parisi, A. Sutera, and Vulpiani, *Tellus* **34**, 10 (1982).
- [3] C. Nicolis and G. Nicolis, *Tellus* **33**, 225 (1981); C. Nicolis, *ibid.* **34**, 1 (1982).
- [4] S. Fauve and F. Heslot, *Phys. Lett.* **97A**, 5 (1983).
- [5] B. McNamara, K. Wiesenfeld, and R. Roy, *Phys. Rev. Lett.* **60**, 2626 (1988).
- [6] B. McNamara and K. Wiesenfeld, *Phys. Rev. A* **39**, 4854 (1989).
- [7] R. Fox, *Phys. Rev. A* **39**, 4148 (1989).
- [8] P. Jung and P. Hänggi, *Europhys. Lett.* **8**, 505 (1989).
- [9] C. Presilla, F. Marchesoni, and L. Gammaitoni, *Phys. Rev. A* **40**, 2105 (1989); L. Gammaitoni, F. Marchesoni, E. Menichella-Saetta, and S. Santucci, *Phys. Rev. Lett.* **62**, 349 (1989); L. Gammaitoni, M. Martinelli, L. Pardi, and S. Santucci, *ibid.* **67**, 1799 (1991).
- [10] T. Zhou and F. Moss, *Phys. Rev. A* **41**, 4255 (1990).
- [11] G. Hu, G. Nicolis, and C. Nicolis, *Phys. Rev. A* **42**, 2030 (1990).
- [12] D. C. Gong, G. Hu, X. D. Wen, C. Y. Yang, G. R. Qing, R. Li, and D. F. Ding, *Phys. Rev. A* **46**, 3243 (1992); G. Hu, D. C. Gong, X. D. Wen, C. Y. Yang, G. R. Qing, and R. Li, *ibid.* **46**, 3250 (1992).
- [13] G. Hu, G. R. Qing, D. C. Gong, and X. D. Wen, *Phys. Rev. A* **44**, 6414 (1990).
- [14] P. Jung and P. Hänggi, *Phys. Rev. A* **44**, 8032 (1991).
- [15] W. M. Zheng, *Phys. Rev. A* **44**, 6443 (1991).
- [16] G. Hu, H. Haken, and C. Z. Ning, *Phys. Lett. A* **172**, 21 (1992).
- [17] H. Risken, *The Fokker-Planck Equation* (Springer, New York, 1985).
- [18] H. Haken, *Synergetics: An Introduction* (Springer, New York, 1983).
- [19] H. Haken, *Advanced Synergetics* (Springer, New York, 1985).